Archives of Biochemistry and Biophysics 519 (2012) 17–22

Contents lists available at SciVerse ScienceDirect

Archives of Biochemistry and Biophysics

journal homepage: www.elsevier.com/locate/yabbi

Characterization of suramin binding sites on the human group IIA secreted phospholipase A_2 by site-directed mutagenesis and molecular dynamics simulation

Elisângela Aparecida Aragão [a], Davi Serradella Vieira [a], Lucimara Chioato [b], Tatiana Lopes Ferreira [b], Marcos Roberto Lourenzoni [c], Samuel Reghim Silva [d], Richard John Ward [a,*]

[a] Department of Chemistry, FFCLRP-USP, Universidade de São Paulo, Brazil
[b] Department of Biochemistry and Immunology, FMRP-USP, Universidade de São Paulo, Brazil
[c] Verdartis – Desenvolvimento Biotecnológico Ltda-ME, SP, Brazil
[d] Computer Science Departament, Universidade Federal de São Carlos, SP, Brazil

ARTICLE INFO

Article history:
Received 19 November 2011
and in revised form 31 December 2011
Available online 10 January 2012

Keywords:
PLA_2 inhibitor
Protein-drug binding
Drug design

ABSTRACT

Suramin is a polysulphonated naphthylurea with inhibitory activity against the human secreted group IIA phospholipase A_2 (hsPLA2GIIA), and we have investigated suramin binding to recombinant hsPLA2GIIA using site-directed mutagenesis and molecular dynamics (MD) simulations. The changes in suramin binding affinity of 13 cationic residue mutants of the hsPLA2GIIA was strongly correlated with alterations in the inhibition of membrane damaging activity of the protein. Suramin binding to hsPLA2GIIA was also studied by MD simulations, which demonstrated that altered intermolecular potential energy of the suramin/mutant complexes was a reliable indicator of affinity change. Although residues in the C-terminal region play a major role in the stabilization of the hsPLA2GIIA/suramin complex, attractive and repulsive hydrophobic and electrostatic interactions with residues throughout the protein together with the adoption of a bent suramin conformation, all contribute to the stability of the complex. Analysis of the hsPLA2-GIIA/suramin interactions allows the prediction of the properties of suramin analogues with improved binding and higher affinities which may be candidates for novel phospholipase A_2 inhibitors.

Introduction

Phospholipases A_2 (PLA_2 – EC 3.1.1.4)[1] catalyze the hydrolysis of the *sn*-2 acyl bonds of *sn*-3 phospholipids [1], and are classified in 16 groups according to amino acid sequence similarity [2]. The human secreted group IIA PLA_2 (hsPLA2GIIA) is found in high concentrations in inflammatory fluids [3] and tears [4], and shows elevated levels of expression in intestinal Paneth cells [5] and macrophages [3,6]. Furthermore, hsPLA2GIIA expression is induced by endotoxins and cytokines, and is generally regarded as a pro-inflammatory protein [7]. The hsPLA2GIIA shows a potent anti-microbial activity against Gram-positive bacteria, in which catalytic [8] and non-catalytic [9] mechanisms contribute to permeabilization of the plasma membrane and cell death. The high number of cationic amino acid residues lends the hsPLA2GIIA a strongly basic character (p*I* = 10.5), and consequently the protein shows hydrolytic activity preferentially against membranes comprised of anionic phospholipids, such as liposome membranes containing lipids with phosphotidylglycerol head-groups and the plasma membrane of Gram-positive bacteria [10,11].

Various compounds reduce the inflammatory effects of PLA_2s by acting as competitive inhibitors [12–15], including indoles [16], oxoamides [17], vitamin E [18] and flavonoids [19]. It has recently been demonstrated that the polysulfonated naphthylurea suramin binds to the hsPLA2GIIA, resulting in the inhibition of catalytic activity and macrophage activation yet without inhibiting the bactericidal effect of the protein [20]. Furthermore, molecular dynamics (MD) simulations of the hsPLA2GIIA/suramin complex together with isothermal titration calorimetry experiments suggested suramin binding is mediated by three regions located on the phospholipid membrane recognition surface of the protein [21]. The location of the suramin binding sites is consistent with the observed inhibition of the phospholipase activity, and represents a novel type of PLA_2/inhibitor interaction. The characterization of new PLA_2 inhibitors leads the development of therapeutic strategies for treatment of pathological processes provoked by these enzymes, and we have therefore extended the mapping of suramin binding sites of the hsPLA2GIIA by site-directed mutagenesis, functional studies of the membrane damaging activity and MD simulations.

* Corresponding author. Address: Departamento de Química, Faculdade de Filosofia, Ciências e Letras de Ribeirão Preto, Universidade de São Paulo, Avenida Bandeirantes, 3900 Monte Alegre, CEP 14040-901, Ribeirão Preto, SP, Brazil. Fax: +55 (0)16 36024838.
E-mail addresses: rjward@fmrp.usp.br, rjward@ffclrp.usp.br (R.J. Ward).

[1] *Abbreviations used:* PLA2, Phospholipase A_2; hsPLA2GIIA, the secreted group IIA human PLA_2; MD, molecular dynamics.

0003-9861
doi:10.1016/j.abb.2012.01.002

Materials and methods

Site directed mutagenesis

The cloning of the full-length cDNA encoding the hsPLA2GIIA (GenBank Accession BC 005919) into the expression vector pET3a has been described previously [20]. Site directed mutagenesis of the hsPLA2GIIA was performed as previously described using PCR mutagenesis [9] to introduce a total of 13 single cationic charge elimination mutations (oligonucleotides used are shown in Table 1). The final PCR fragments were cloned into the expression vector pET3a and fully sequenced. After expression as inclusion bodies in *Escherichia coli* BL21, the proteins were refolding and purified as previously described [20].

Suramin binding by intrinsic suramin fluorescence emission

Wild-type hsPLA2GIIA or mutants at a concentration of 3 μM were titrated with suramin (Sigma–Aldrich, St. Louis, MO, USA) over the concentration range 0–100 μM in a buffer containing 20 mM NaH_2PO_4, 150 mM NaCl, pH 7.2. The changes in intrinsic suramin fluorescence emission were measured with a Spectronic SLM 8100C spectrofluorimeter at 25 °C, using a stirred 1 cm optical path length quartz cuvette. The samples were excited at 350 nm and the emission spectrum was measured between 375 and 500 nm. Suramin absorbance at 350 nm leads to an inner filter effect, therefore the fluorescence emission intensities were corrected using a molar extinction coefficient of 7060 $cm^{-1}\,M^{-1}$ as derived from an appropriate suramin calibration curve. After normalization of the fluorescence emission signal, the equilibrium dissociation constant (K_D) for each suramin/protein complex was estimated by nonlinear curve fitting with a sigmoidal dose–response function using the OriginPro 8 software (OriginLab Corporation, Northampton, MA, USA).

Effect of suramin on the Ca^{2+} independent membrane damaging activity of the hsPLA2GIIA

The Ca^{2+}-independent membrane damaging activity was evaluated by the fluorescence increase due to the release of the liposome entrapped self-quenching fluorescent dye calcein. Unilamellar liposomes composed of dioleoyl phosphatidylcholine (DOPC – Sigma–Aldrich, St. Louis, MO, USA) and dioleoyl phosphatidylglycerol (DOPG – Sigma–Aldrich, St. Louis, MO, USA) at a 1:1 M ratio containing 25 mM calcein (Sigma–Aldrich, St. Louis, MO, USA) in buffer containing 20 mM Hepes, 20 mM NaCl were prepared by reverse phase evaporation [22]. Suramin at a concentration of 0.75 μM was pre-incubated for 15 min with 4 μg/mL of $hsPLA_2GIIA$ or mutants, and added to the liposome to a final protein:lipid molar ratio of 1:200. Membrane damage induced by the protein was monitored by the increase in fluorescence emission at 520 nm with excitation at 490 nm, and the signal was expressed as the percentage of total calcein liberation on addition of 5 mM Triton X-100. The effect of suramin was measured in five independent experiments, and the data were analyzed using ANOVA with a subsequent Tukey test.

Table 1
Oligonucleotide sequences of primers used for the generation of the charge elimination site-directed mutants of the hsPLA2GIIA.

R7A	TGATCATTGCGTGGAAATT
K15A	GCGGCTTCCGCTCCTGTCGT
K38A	CCGTTGCATCCGCGGGGGATCC
H48Q	AGCAACAGTCGTTAGTGACACA
D49K	GTAGCAACATTTATGAGTGACACA
K53A	CCAGACGTGCGTAGCAACA
R54A	CTCCAGAGCTTTGTAGCA
K57A	CCACGTGCCTCCAGACG
R58A	GCCACATCCAGCTTTCTCCAG
ΔK57/R58	GGTGCCACATCCACGTTTCTCCAGACGTTTGTA
K115A	GGTACTTTGCATTGTAGGT
K116A	ACTGGTACGCTTTATTGTA
K123A	CTGCAGTGTGCATTGGAATA

All sequences are shown in the 5′–3′ direction, and the underlined bases indicate the codon that was introduced during the mutagenesis.

Molecular dynamics simulations of the $hsPLA_2GIIA$/complex

All MD simulations were carried out using the GROMACS 4.5 software package [23] and the GROMOS-96 (43A2) force field [24] in constant volume (NVT ensemble) using the "leapfrog" algorithm [25] with a time step of 2.0 fs. The systems for MD simulations were constituted by 16,500 SPC water molecules [26], a monomer of $hsPLA_2GIIA$ (PDB code 1POE, [27]) and a single suramin molecule. A cubic simulation box was adjusted to give a density of 0.997 kg L^{-3} for the water molecules. The initial suramin localization on the surface of the $hsPLA_2GIIA$ was made by a 20 ns extension of the previously described simulation of the $hsPLA_2GIIA$/complex using the same parameters [21]. The mutants R7A, R58A, K116A and ΔK57/R58 (a mutant in which residues K57 and R58 are deleted) were also investigated by MD simulations. The initial configurations for these mutants were based on the simulated structure of wild-type $hsPLA_2GIIA$/suramin complex [21], in which the particular mutation under study had been introduced. All the simulations were run with the total time of 20 ns and the atomic trajectories were sampled each 40 ps. The long-range interactions were treated using the particle-mesh Ewald sum (PME) method [28] and calculated with a cutoff of 1.4 nm, and the intermolecular Interaction Potentials (IIP) were computed within the same cutoff distance. Electrostatic potential surfaces around wild-type hsPLA2GIIA and mutants/suramin complexes were calculated with the Poisson–Boltzmann equation with APBS [29] and PDB2PQR [30].

Results and discussion

Scanning alanine mutagenesis of 13 cationic residues has been used to evaluate the mapping of the suramin binding sites on the hsPLA2GIIA. Dideoxynucleotide sequencing of all 13 mutants confirmed that the only differences observed between the wild-type and mutant hsPLA2GIIA coding sequences were those introduced during the mutagenesis procedure. The far ultraviolet circular dichroism spectra of all mutants (Supplementary Fig. S1) present a spectral profile that is similar to the wild-type hsPLA2GIIA with minima at 209 and 222 nm, which are typical of proteins that are rich in α-helical structure, and are similar to those previously reported for the recombinant hsPLA2GIIA [9,20]. The results demonstrate that the refolding and purification procedures yielded wild-type and mutant proteins with native-like secondary structure.

The polysulphonated naphthylurea suramin has a long history of use as an antiprotozoal and anthelminitic drug [31,32], and more recently has attracted interest due to its antineoplastic and antiangiogenic activities (see the discussion in [20] for a brief review of the recent literature). As a polyanion, suramin forms stable interactions with cationic surfaces of basic proteins [33,34], and in the present study suramin binding to the hsPLA2GIIA and mutants was evaluated by changes in the intrinsic suramin fluorescence intensity. Fig. 1 shows that on suramin binding, the suramin intrinsic fluorescence emission at 440 nm increases in a sigmoid manner for all proteins. The equilibrium dissociation constant (K_D) for all

proteins estimated from least squares fitting of the binding data is shown in Supplementary Table S1. The wild-type hsPLA2GIIA presents a K_D of 6.3 μM, and the suramin affinity of the hsPLA2GIIA was significantly reduced by the mutations K15A (located in the N-terminal, K_D = 28.4 μM), R54A (close to the active site, K_D = 12.5 μM) and K123A (in the C-terminal loop region, K_D = 9.7 μM). These results suggest that these three regions of the protein contribute to binding the suramin. In contrast, the mutants D49K (active site, K_D = 3.3 μM), ΔK57/R58 (hydrophobic substrate binding channel, K_D = 2.1 μM) and K116A (C-terminal loop, K_D = 3.8 μM) increased the suramin affinity relative to the wild-type protein.

We have recently demonstrated that in addition to its Ca^{2+}-dependent hydrolytic activity, the hsPLA$_2$GIIA also displays a Ca^{2+}-independent membrane damaging activity [9]. The Ca^{2+}-independent membrane permeabilizing activity was evaluated by measuring the calcein release from liposomes comprised of mixed DOPC/DOPG phospholipids, which is a lipid mixture that has been previously used to study the mechanism of action of the hsPLA$_2$-GIIA [9,35]. Fig. 2A presents the percentage of calcein release by wild-type and mutant hsPLA2GIIA both in the absence of suramin and after incubation with suramin at a concentration of 0.75 μM. In the absence of suramin, no significant differences in the Ca^{2+}-independent membrane permeabilizing activity were observed between the wild-type and the mutant proteins (Fig. 2A – light grey bars). Under the chosen conditions suramin inhibits approximately 50% of the calcein release caused by the wild-type hsPLA2-GIIA, and reduces the Ca^{2+}-independent membrane permeabilizing activity of all mutants (Fig. 2A – dark grey bars). The inhibition of the membrane damaging effect by suramin was quantified as the percentage reduction in the calcein release in the presence of suramin as compared to the effect in the absence of suramin (see Fig. 2B). The inhibitory effect of suramin in relation to wild-type protein was reduced in the R7A, K15A, R54A, R58A and K123A mutants, and enhanced in the H48Q, D49K and K116A mutants.

Comparison of the results of the liposome membrane damaging activity assays with those from the suramin binding experiment shows a strong correlation. The mutants K15A, R54A and K123A, which have reduced suramin affinities, also present a reduced inhibition of the calcein release from liposomes. In contrast, the mutants H48Q and D49K (located in the active site region of the protein) and K116A (located in the C-terminal region), all of which present an increased affinity for suramin, were inhibited to a greater degree in relation to the wild-type protein. Finally, the mutants R7A, R58A and ΔK57/R58 showed no correlation between affinity and suramin inhibition. To gain further insights as to underlying structural basis of these results, molecular dynamics simulations were performed on hsPLA2GIIA/suramin and R58A, ΔK57/R58 and K116A mutant/suramin complexes.

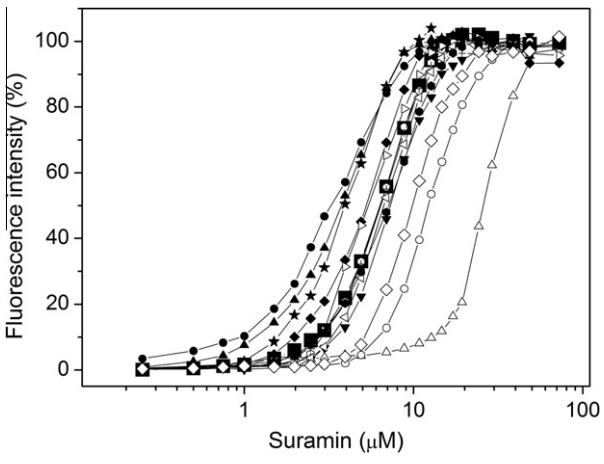

Fig. 1. Suramin fluorescence intensity changes on interaction with the wild-type hsPLAGIIA and mutant proteins. Suramin binding to the hsPLAGIIA and mutants was evaluated by the increase in intrinsic suramin fluorescence emission at 440 nm. The curves show fluorescence changes on titration of the wild type hsPLAGIIA (solid squares) and mutants R7A (open circles), K15A (open up triangles), K38A (solid down triangles), H48Q (solid diamonds), D49K(solid up triangles), K53A (crosses), R54A (open hexagons), K57A (open right triangles), R58A (open left triangles), ΔK57/R58 (solid circles), K115A (solid hexagons), K116A (solid stars) and K123A (open diamonds). See materials and methods for further experimental details.

Molecular dynamics (MD) simulations

Based on the electrostatic properties of both the hsPLA2GIIA and suramin, three possible suramin binding regions on the membrane recognition surface of the protein have been previously been proposed [21]. Analysis of the hsPLA2GIIA/suramin complex in MD simulations suggested two alternative conformations of the bound suramin involving three regions on the protein; (1) the substrate binding/active-site region, (2) residues in the N-terminal region, and (3) residues in the C-terminal region of the protein [21]. Although these previous results corroborate the experimental data obtained in the present work, the unexpected properties of some mutants prompted us to investigate the suramin binding to the hsPLA2GIIA in more detail by MD simulations of suramin complexes with mutants that either maintained (R58A) or increased (ΔK57/R58, K116A) the affinity as measured by the changes in intrinsic suramin fluorescence.

MD simulations provide a trajectory of atomic positions, and calculation of the Intermolecular Interaction Potential (IIP) between the hsPLA2GIIA and the suramin allows the direct evaluation of the stability of the hsPLA2GIIA/suramin complex in aqueous solution. Reliable IIP calculations depend on an ensemble of hsPLA2GIIA and suramin structures generated by MD that are at equilibrium, which is properly evaluated by calculation of the root mean square deviations (RMSD) from the initial structure for all protein Cα atoms. The IIP and RMSD averages were computed over the 20 ns trajectories, and the average RMSD(t) values for the protein Cα atoms in the simulated complexes are 0.24 ± 0.02 nm (hsPLA$_2$gIIA), 0.23 ± 0.03 nm (R58A), 0.17 ± 0.02 nm (ΔK57/R58) and 0.22 ± 0.04 nm (K116A). These results indicate that the hsPLA2GIIA structures are not significantly altered either as a consequence of the mutations or as a result of suramin binding.

The IIP per residue in the protein/suramin complexes can provide further insights as to the contributions of individual residues to the interaction potential. Fig. 3 shows IIP per residue for the hsPLA2GIIA and mutant proteins, where residues which present a negative IIP are those with attractive interactions with the suramin molecule, and those residues that have positive potentials contribute to repulsive interactions. For example, residue R54 is located close to the C-terminal region of the protein and due to the proximity of the suramin sulphonate groups presents an average intermolecular potential energy value of -74.8 kJ mol^{-1}. The value of the potential varies over the range of −69.00 to −80.00 kJ mol^{-1}, and this residue can therefore be considered to make a significant contribution to suramin binding, and readily explains the observed reduction in the hsPLA$_2$gIIA/suramin affinity of the K54A mutant. Table 2 presents the IIP for selected residues that present highly attractive interactions in different mutants, and which can be considered as component of suramin binding sites. Residues R7, K10 and K15 are located in the N-terminal region and K115, K116 and K123 in the C-terminal region, and all residues show different IIP values between the different mutants. This demonstrates that the contribution of a given residue to the formation of different mutant/suramin complexes is not necessarily constant, and is

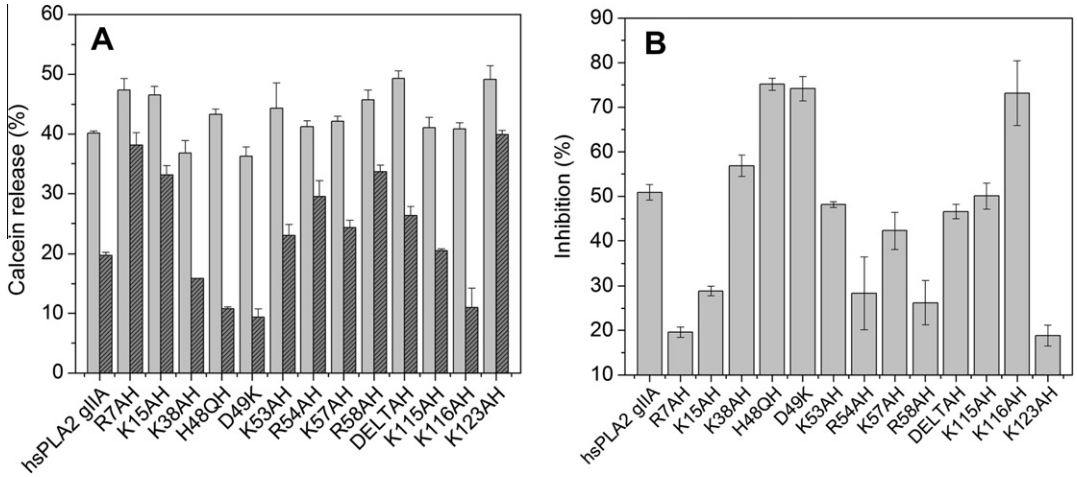

Fig. 2. (A) The effect of suramin on the membrane-damaging activity of the wild-type hsPLA2GIIA and mutants as measured by the release of the encapsulated fluorescent marker calcein from DOPC:DOPG liposomes. (B) Percentage inhibition by suramin of the membrane-damaging activity of the hsPLA2GIIA and mutants. Calcein liberation is expressed as the percentage of total marker release after addition of 5 mM Triton X-100. Results are presented as the mean ± SD (n = 3). The mutants R7A, K15A, R54A, R58A and K123A significantly reduced the activity ($p < 0.05$) in relation to the wild-type protein.

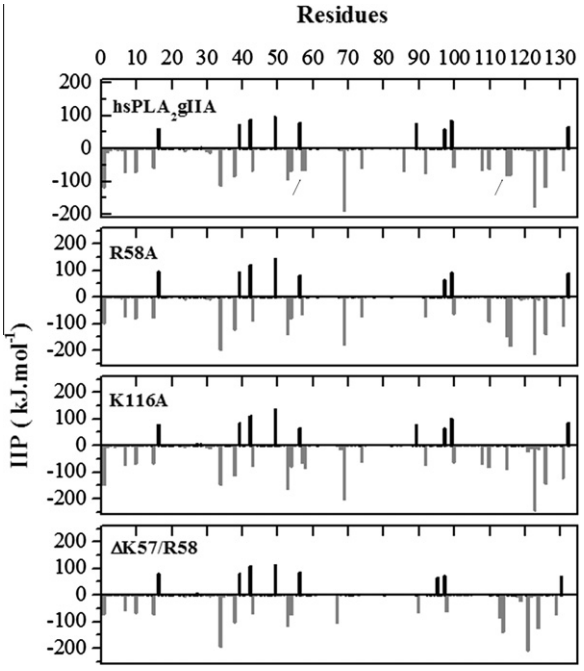

Fig. 3. Intermolecular Interaction potential per residue of suramin/hsPLA2GIIA and suramin/mutant complexes calculated from 20 ns MD trajectories. The arrows indicate positions 7 (left), 57 and 58 (middle), 115 and 116 (right).

influenced by neighboring residues which contribute to the local surface potential.

The IIP between suramin and the hsPLA2GIIA or mutants is -619 ± -90 kJ mol^{-1}, which compares with values of -642 ± -92 kJ mol^{-1} (R58A/suramin), -837 ± -80 kJ mol^{-1} (ΔK57/R58/suramin) and -865 ± -79 kJ mol^{-1} (K116A/suramin), demonstrating that the elimination of cationic residues at these different positions resulted in a more attractive interaction between the hsPLA2GIIA and suramin. The lowest IIP were calculated for the ΔK57/R58 and K116A and would predict a higher suramin affinity for these mutants, which indeed is corroborated by the experimental measurements.

The electrostatic potential at the molecular surfaces of the complexes between suramin and the wild-type hsPLA2GIIA and mutants are shown in Fig. 4. The potential at the surface of the protein varies between the mutants, and consequently the bound suramin molecule undergoes conformational changes in order to optimize the docking of the sulphonate groups to the protein surface. In all mutants, the more hydrophobic central region of the suramin molecule fits within the hydrophobic substrate-binding/active-site of the protein, a situation that is not observed in wild-type hsPLA2GIIA. Furthermore, the suramin adopts a bent conformation with one of its ends oriented directly towards the C-terminal loop, while the other end is closer to the region of the catalytic site and residues 57 and 58 on one of the long α-helices. The conformations of the bound suramin that are observed in the present study were not detected in previous investigations [21], which suggest that the altered surface potential resulting from mutations in the hsPLA2GIIA can lead to variation in the optimal conformation of the bound suramin.

The IIP results presented in Fig. 3 and in Table 2 together with the electrostatic potential molecular surfaces presented in Fig. 4 provide a virtual contact map of the attractive and repulsive

Table 2
Intermolecular interaction potential (IIP) for residues in the N- and C-terminal sites. The values are given in kJ/mol. In case of ΔK57/R58, the residues K115, K116 and K123 are the K113, K114 and K121 due to deletion of two residues.

RESIDUE	hsPLA2GIIA	K116A	R58A	R7A	ΔK57/R58
R7	69.5 ± 18.9	−71.8 ± 7.0	−73.4 ± 5.4	−1.73 ± 0.43	−54.9 ± 15.0
K10	−71.6 ± 21.0	−69.5 ± 10.0	−79.3 ± 5.7	−84.2 ± 7.42	−66.9 ± 15.0
K15	−58.2 ± 15.0	−67.9 ± 8.1	−77.4 ± 14.7	−80.6 ± 10.4	−72.2 ± 17.2
K115	−81.5 ± 21.8	−87.2 ± 29.2	−147.6 ± 43.1	−83.3 ± 13.6	−86.4 ± 26.2
K116	−79.4 ± 29.3	3.81 ± 0.96	−184.6 ± 59.1	−149.3 ± 42.2	−139.5 ± 51.3
K123	−177.2 ± 59.7	−243.4 ± 40.1	−214.4 ± 28.3	−220.2 ± 28.2	−230.5 ± 56.1

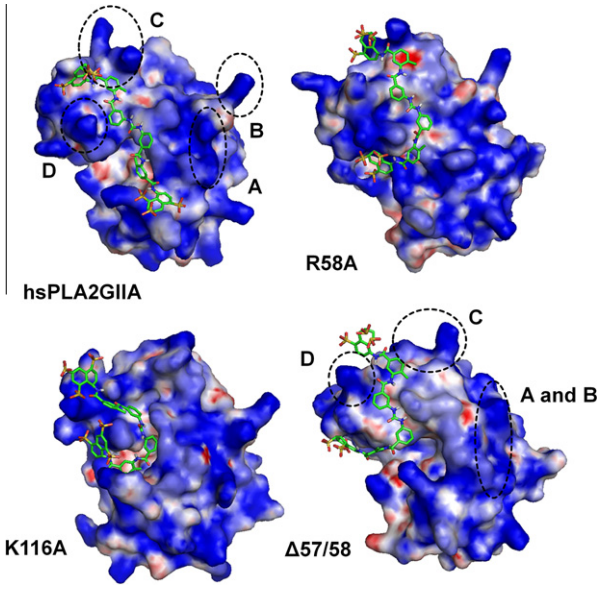

Fig. 4. Electrostatic potential molecular surfaces of representative structures obtained from MD trajectories of suramin complexes with the wild-type hsPLA2GIIA and the mutants R58A, K116A and Δ57/58. The localization of residues R7 and K10 (labeled A) and K15 (labeled B) contribute to the main interaction sites on the N-terminal, and the residues of the main interaction sites on C-terminal are K115 and K116 (labeled C) and K123 (labeled D). The localizations of the residues with high repulsive intermolecular potential energy are shown in red and blue for the closest to, and more distant from, the suramin molecule. Contour levels are in dimensionless units of −10kT/*e* (red) to 10kBT/*e* (blue), where k is the Boltzmann's constant, T is the temperature in Kelvin and *e* is the elementary charge. (For interpretation of the references to colour in this figure legend, the reader is referred to the web version of this article.)

suramin contacts with the hsPLA2GIIA and mutants from which the changes in the affinity can be predicted. The data in Table 2 show that the IIP between the selected residues and the suramin changes depending on the mutation in the hsPLA2GIIA. Residues in the N-terminal region (R7, K10 and K15) show little variation in the IIP, indicating that these positions are insensitive to the effects of the mutations. In contrast, residues in the C-terminal loop (K115, K116 and K123) showed a significant reduction in the IIP. The K115 residue is only sensitive to the R58A mutation, which resulted in an increased in the attractive interaction with the suramin. In the case of the K116 residue, more attractive interactions with suramin were observed in the R58A, R7A and ΔK57/R58 mutants. Finally, the K123 residue shows an enhanced IIP with suramin in all mutants, especially in the case of the K116A mutation. This shows that within the C-terminal region, the attractive interaction of the K123 residue with the suramin is particularly influenced by the K116 residue, and this the difference in the suramin conformation in the K116A mutant, whose position is closer to the K123 residue than the other mutants (Fig. 4).

The main sources of repulsion in the hsPLA2GIIA/suramin complexes (shown as positive potentials in Fig. 3) include the negatively charged residues E16, G38, D41, D48, E55, D81, E89 and D91, which present variations in intermolecular potential energy from +80 to +100 kJ mol^{-1}. These residues can be divided into two groups, the first (A and B in Fig. 4) are located in the α-helix more distant from suramin molecule and the second (C and D) are located closer to the suramin molecule. This information could be useful for the design of new hsPLA2GIIA inhibitors based on the chemical structure of suramin, where we suggest the maintenance of a high density of negative charges at the extremities but a reduced negative charge in the central region of the molecule. Furthermore, shortening of the central region of the suramin molecule by removing one or two rings could facilitate a bent conformation of the bound molecule that optimizes contact with C-terminal region of the hsPLA2GIIA.

In conclusion, site-directed mutagenesis of the cationic residues of the hsPLA2GIIA had variable effects on the affinity of suramin for the protein. In those mutants that showed increased suramin affinity, a significant conformational change of the suramin molecule was observed as a result of the modified potential surface of the protein induced by mutations, which was unrelated to any of the suramin conformations previously observed in the hsPLA2GIIA/suramin complex. In the case of K116A and ΔK57/R58 mutants, the suramin molecule presented a bent conformation favoring interactions with residues in the C-terminal region. We conclude that the C-terminal region is crucial to the stabilization of the hsPLA2GIIA/suramin complex and consequently is a major structural determinant of the inhibitory action of suramin. We suggest that mutations which modify the potential surface of the protein may also promote a bent suramin conformation, which increases the complex stability. In addition to contributing to the understanding of hsPLA2GIIA/inhibitor interactions, the present study has demonstrated the viability of using MD simulations not only for the interpretation of experimental results, but also for the design of new compounds for hsPLA2GIIA inhibitors that are based on the suramin molecule.

Acknowledgments

EAA and TLF were recipients of FAPESP fellowships 2009/13902-7 and 2002/12746-2, DSF and MRL were beneficiaries of CNPq fellowships 152669/2007-8 and 504807/2009-9. The work was supported by CNPq stipend 304982/2006-7 and PRP-USP.

Appendix A. Supplementary data

Supplementary data associated with this article can be found, in the online version, at doi:10.1016/j.abb.2012.01.002.

References

[1] L.L.M. van Deenen, G.H. de Haas, Biochem. Biophys. Acta 70 (1963) 538–553.
[2] R.H. Schaloske, E.A. Dennis, Biochem. Biophys. Acta 1761 (2006) 1246–1259.
[3] P. Vadas, J. Browning, J. Edelson, W. Pruzanski, J. Lipid Mediators 8 (1993) 1–30.
[4] X.D. Qu, R.I. Lehrer, Infect. Immun. 66 (1998) 2791–2797.
[5] S.S. Harwig, L. Tan, X.D. Qu, Y. Cho, P.B. Eisenhauer, R.I. Lehrer, J. Clin. Invest. 95 (1995) 603–610.
[6] M. Murakami, Y. Nakatani, G. Atsumi, K. Inoue, I. Kudo, Crit. Rev. Immunol. 17 (1997) 225–283.
[7] R.M. Crowl, T.J. Stoller, R.R. Conroy, C.R. Stoner, J. Biol. Chem. 266 (1991) 2647–2651.
[8] S.A. Beers, A.G. Buckland, R.S. Koduri, W. Cho, M.H. Gelb, D.C. Wilton, J. Biol. Chem. 277 (2002) 1788–1793.
[9] L. Chioato, E.A. Aragao, T.L. Ferreira, R.J. Ward, Biochimie 94 (2012) 132–136.
[10] A.G. Buckland, E.L. Heeley, D.C. Wilton, Biochim. Biophys. Acta 1484 (2000) 195–206.
[11] V.J. Laine, D.S. Grass, T.J. Nevalainen, J. Immunol. 162 (1999) 7402–7408.
[12] E.A. Dennis, J. Cao, Y.H. Hsu, V. Magrioti, G. Kokotos, Chem. Rev. 111 (2011) 6130–6185.
[13] V. Magrioti, G. Kokotos, Anti-Inflamm. Anti-Allergy Agents Med. Chem. 5 (2006) 189–203.
[14] V. Magrioti, G. Kokotos, Exp. Opin. Therap. Patents 20 (2010) 1–18.
[15] R.C. Reid, Curr. Med. Chem. 12 (2005) 3011–3026.
[16] P. Bernard, M. Pintore, J.Y. Berthon, J.R. Chretien, Eur. J. Med. Chem. 36 (2001) 1–19.
[17] V.D. Mouchlis, V. Magrioti, E. Barbayianni, N. Cermak, R.C. Oslund, T.M. Mavromoustakos, M.H. Gelb, G. Kokotos, Bioorg. Med. Chem. 19 (2011) 735–743.
[18] A.P. Pentland, A.R. Morrison, S.C. Jacobs, L.L. Hruza, J.S. Hebert, L. Packer, J. Biol. Chem. 267 (1992) 15578–15584.
[19] J. Lattig, M. Bohl, P. Fischer, S. Tischer, C. Tietbohl, M. Menschikowski, H.O. Gutzeit, P. Metz, M.T. Pisabarro, J. Comput. Aided Mol. Des. 21 (2007) 473–483.
[20] E.A. Aragao, L. Chioato, T.L. Ferreira, Inflamm. Res. 58 (2009) 210–217.
[21] D.S. Vieira, E.A. Aragao, M.R. Lourenzoni, R.J. Ward, Bioorg. Chem. 37 (2009) 41–45.
[22] T.L. Ferreira, R. Ruller, L. Chioato, R.J. Ward, Biochimie 90 (2008) 1397–1406.

[23] B. Hess, C. Kutzner, J. Chem. Theory Comput. 4 (2008) 435–447.
[24] L.D. Schuler, X. Daura, W.F. van Gunsteren, J. Comp. Chem. 22 (2001) 1205–1218.
[25] R.W. Hockney, S.P. Goel, J. Comp. Phys. 14 (1974) 148–158.
[26] H.J.C. Berendsen, J.P.M. Postma, W.F. van Gunsteren, J. Hermans, Interactions models for water in relation to protein hydration, Reidel Publishing Company, Dordrecht, 1981.
[27] D.L. Scott, S.P. White, J.L. Browning, J.J. Rosa, M.H. Gelb, P.B. Sigler, Science 254 (1991) 1007–1010.
[28] T. Darden, D. York, L. Pedersen, J. Chem. Phys. 98 (1993) 10089–10092.
[29] N.A. Baker, D. Sept, S. Joseph, M.J. Holst, J.A. McCammon, Proc. Natl. Acad. Sci. USA 98 (2001) 10037–10041.
[30] T.J. Dolinsky, J.E. Nielsen, J.A. McCammon, N.A. Baker, Nucleic Acids Res. 32 (2004) W665–667.
[31] J.K. Cherry, East Afr. Med. J. 37 (1960) 550–558.
[32] J. Schneider, Bull. World Health Organ 28 (1963) 763–786.
[33] M. Freissmuth, S. Boehm, W. Beindl, P. Nickel, A.P. Ijzerman, M. Hohenegger, C. Nanoff, Mol. Pharmacol. 49 (1996) 602–611.
[34] M. Freissmuth, M. Waldhoer, E. Bofill-Cardona, C. Nanoff, Trends Pharmacol. Sci. 20 (1999) 237–245.
[35] S.A. Beers, A.G. Buckland, N. Giles, M.H. Gelb, D.C. Wilton, Biochemistry 42 (2003) 7326–7338.